

A microscopic image of tissue, likely a histological section, showing a dense population of cells. The cells are stained with a blue dye, possibly hematoxylin, and a red dye, possibly eosin. The red staining highlights certain structures, possibly connective tissue or specific cell components. The overall appearance is a complex, textured pattern of blue and red against a dark background.

Using Annotated PDFs to Streamline the Revision Process

Allen Press Editorial Seminar
Thursday, October 4, 2007, 2:15-3:15 p.m.

Melissa Clifton
Deputy Managing Editor
Biology of Reproduction

Introduction

- Why
- Problems
- Tricks & Tips
- Impact

Time and Money

- Implement a 45-day schedule
- Reduce shipping costs
- Appease savvy Authors

Authors to Journal Office

- Author downloads galley proof from AP FTP site
- Author notifies journal that PDF has been downloaded (within 48 hours)
- Author returns corrections
- Staff check corrections and queries
- Staff annotate PDF

Journal Office to Allen Press

- FTP download of galley proof
- Change file name
- Move to new folder
- Make (annotate) corrections onto PDF
- When ready, move to the day's FTP folder
- FTP back to AP
- Notify account manager of FTP

Author Corrections

How do they send them? Let me count the ways...

1. Fax
2. Email
3. Annotated PDF “light”
4. Annotated PDF “hardcore”
5. And, yes, even by FedEx or USPS!

Problems

- A nice, daily workflow, right?
- Not everyone has the same tools (versions, formats, etc.)
- Authors are not the best annotators

are few reports about the mechanism of the regulation of early development of mouse fertilized eggs, especially the events of entry into M-phase. Here we report that AKT causes the activation of MPF and strongly promotes the development of one-cell stage mouse fertilized eggs by inducing AKT-dependent phosphorylation of CDC25B, a member of CDC25 phosphatase family. Our findings identify CDC25B as a potential target of AKT and provide new insight into the effect of AKT in the regulation of mouse early embryo development.

MATERIALS AND METHODS

Animals and Reagents

Kunming strain mice were obtained from the Department of Laboratory Animals, China Medical University (CMU). All experiments were performed at CMU in accordance with the NIH Guidelines for the Care and Use of Laboratory Animals. The protocol for animal handling and the treatment procedures were reviewed and approved by the CMU Animal Care and Use Committee. Reagents, unless otherwise specified, were from Sigma.

Collection and Culture of Mouse Embryos

One-cell stage mouse embryos were collected and cultured according to the method described by Hogan and Constantini [25]. Female mice at 4–6 wk old were abnormally injected with 10 IU of eCG and 48 h later with 10 IU hCG. A single female was placed with a single male for fertilization. One-cell embryos were collected with M2 medium the next day (20 h after hCG injection) from the oviduct of females possessing a vaginal plug. After injection with mRNA, embryos were cultured in a drop of M16 medium under paraffin oil at 37°C in a humidified atmosphere of 5% CO₂ in air.

Construction of mRNA Expression Vectors

The constructs encoding the wild-type AKT (pCIS2-Akt1-WT), myristoylated AKT (pCIS2-myr-Akt1) and kinase-deficient AKT (pCIS2-Akt1-KD) were gifts from Michael J. Quon (National Institutes of Health) [26, 27].

The coding sequences of wild-type AKT (Akt1-WT), kinase-deficient AKT (Akt1-KD), and myristoylated AKT (myr-Akt1) were amplified by PCR using the pCIS2-Akt1-WT, pCIS2-Akt1-KD, and pCIS2-myr-Akt1, respectively, as templates and introduced the enzyme-incision site of *Hind*III and *Bam*HI into 5' and 3' end respectively. The products were cloned into the mRNA expression vector pcDNA3.1/myc-His B (Invitrogen) and named pcDNA3.1-Akt1-WT, pcDNA3.1-Akt1-KD, and pcDNA3.1-myr-Akt1. The pBSK-Cdc25b-WT was subcloned into pcDNA3.1/myc-His B using *Kpn*I and *Bam*HI. The recombinant was called pcDNA3.1-Cdc25b-WT.

A Site-Directed Mutagenesis Kit (Stratagene) was used to mutate Ser351 to a nonphosphorylatable alanine of CDC25B, and this mutant was called pcDNA3.1-Cdc25b-S351A.

All the above recombinant plasmids were sequenced to verify the correct gene insertion and successful mutation and were used as templates for *in vitro* transcription.

In Vitro Transcription

All the constructs in pcDNA3.1/myc-His B were cut singly with *Age*I and transcribed *in vitro* into 5'-capped mRNA for microinjection by using the mMESSAGE mMACHINE kit (Ambion). The *in vitro*-synthesized mRNA was dissolved in nuclease-free 5 mM Tris and 0.5 mM EDTA (TE; pH 7.4). We determined mRNA yield by measuring absorbance at 260 nm and by carrying out modified nondenaturing gels loaded with RNA.

mRNA Microinjection and Observation of the Mouse Embryos

Various mRNA were injected into one-cell stage embryos at G2 phase using a micropipette and Eppendorf TransferMan manipulators mounted on an Olympus IX-70 inverted microscope with DIC optics. Eggs were placed in a drop of M2 medium under paraffin oil in the lid of a 3-cm Falcon culture dish. Typical injection volume was 5% of total cell volume or 10 μ l per egg. Messenger RNA was diluted to various concentrations in TE buffer (pH 7.4) without nuclease contaminant. Eggs in control groups were either not microinjected or microinjected with TE buffer. The percentages of cell division

and cell survival were counted under a dissecting microscope 30 h and 35 h after injection of hCG, and the results were analyzed statistically.

Assay of MPF Activity

MPF kinase activity was measured using histone H1 kinase assay [28]. Five eggs cultured in M16 medium were collected, washed in collection buffer (PBS containing 1 mg/ml polyvinyl alcohol, 5 mM EDTA, 10 mM Na₂VO₄, and 10 mM NaF), and then transferred to an Eppendorf tube containing 5 μ l of the collection buffer. The Eppendorf tube was immediately stored at -70°C until the kinase assay was performed.

The frozen eggs were thawed and subjected to freezing and thawing three times. A total of 25 μ l of MPF buffer (54 mM β -glycerophosphate, 14.5 mM p-nitrophenylphosphate, 24 mM 3-(N-morpholino)-propanesulfonic acid [MOPS; pH 7.2], 14.5 mM MgCl₂, 14.5 mM ethyleneglycoltetraacetic acid, 0.12 mM EDTA, 1 mM dithiothreitol [DTT], 2.4 μ M PKA inhibitor peptide [PKI], 75 mM genistein [a tyrosine kinase inhibitor], 10 μ M ML-9 [a myosin light chain kinase inhibitor], 1 mg/ml histone H1 [type III-s], and 1 mg/L each of leupeptin, aprotinin, pepstatin, chymostatin, and trypsin-chymotrypsin inhibitor) was then added to the disrupted cells. The histone H1 kinase reaction was started by adding 25 μ l of 20 μ Ci/ml [γ -³²P]ATP incubated at 30°C for 10 min. Then 25- μ l aliquots were spotted on Whatman p81 paper, and the reaction was stopped with 5% H₃PO₄ solution. After thorough washing, the radioactivity on the filter paper was counted with a BECKMAN scintillation counter.

A parallel incubation was performed to confirm the phosphorylation of histone H1. Protein extract from 10 oocytes was incubated with 50 μ l of MPF buffer containing 50 μ Ci/ml [γ -³²P]ATP at 37°C for 30 min, and the reaction was stopped by adding an equal amount of 2 \times SDS buffer. The reaction was then resolved on a 12% SDS-PAGE gel, and the incorporation of ³²P into histone H1 was visualized by autoradiography.

Assay of PKB Activity

Ten eggs cultured in M16 medium were collected and lysed as described above and assayed for 30 min at room temperature in AKT reaction buffer containing 50 mM Hepes (pH 7.5), 10 mM MgCl₂, 1 mM DTT, 1 μ M PKI, 40 μ Ci/ml [γ -³²P]ATP, and 0.2 mg/ml histone H2B used as substrate. AKT activity was also determined by scintillation counting and autoradiography, as in the MPF activity assay.

Western Blotting

Protein extracts of mouse fertilized eggs were prepared by adding approximately 150 eggs in a minimal volume of collection medium to 20 μ l of protein extraction buffer (100 mM NaCl, 20 mM Tris-HCl [pH 7.5], 0.5% Triton X-100, 0.5% NP-40) containing 1 mM phenylmethylsulfonyl fluoride and 1 μ g/ml leupeptin and pepstatin. Laemmli sample buffer was added to the protein extracts, and the mixture was boiled for 5 min and resolved on a 12% SDS-PAGE gel. For immunoblotting, the fractionated proteins were transferred to a nitrocellulose membrane. The membrane was blocked with 3% BSA in Tris-buffered saline containing 0.05% Tween 20 and probed with primary antibodies in a sealed plastic bag at 4°C overnight. The primary antibody against pTyr15 of CDC2A or CCNB1 (Santa Cruz Biotechnology) was used at 1:400 dilution, or the anti-MYC antibody (Invitrogen) used at 1:1000 dilution.

The membrane was then incubated with alkaline phosphatase-conjugated anti-mouse IgG secondary antibody at 1:3000 (Beijing Zhongshan Biotechnology). The proteins were detected by using O-dianiline and β -naphthyl acid phosphate as the substrates of alkaline phosphatase.

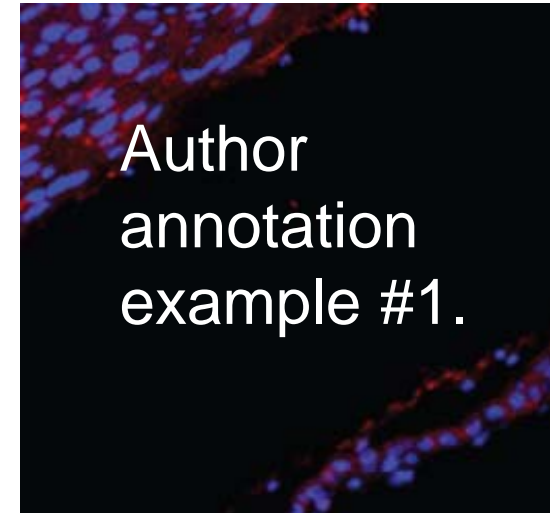
Statistical Analysis

One-way analysis of variance or Student *t*-test was used to evaluate the difference between groups, and differences at *P* < 0.05 were considered to be significant. SPSS 13.0 software was used to perform statistical analyses.

RESULTS

AKT mRNA Microinjection Interferes with Cell Division of One-Cell Stage Mouse Fertilized Eggs

To test whether AKT kinase activity and the membrane targeting are involved in the mitotic cell cycle of fertilized eggs, three AKT constructs encoding Akt1-WT, myr-Akt1, and Akt1-KD were used in our experiment. In the myr-Akt1 construct, the AKT coding region is fused to a myristoylation



Author
annotation
example #1.

enzymes involved in the synthesis of seminolipid or of its immediate precursor result in impaired spermatogenesis [45, 46]. Cerebroside sulfotransferase (CST)-null mice, generated by gene targeting, have been used to show that the same enzyme is involved in the synthesis of both brain sulfogalactosylceramide and testicular seminolipid [46]. *Cst(-/-)* mice lack the former lipid in the brain and the latter lipid in the testis. Notably, whereas *Cst(-/-)* mice of both sexes show neurological abnormalities, only the males are infertile due to a block in spermatogenesis before the first meiotic division [46], which underlines the essential nature of seminolipid in normal spermatogenesis. In the present study, the fact that cryptorchidism induced the total loss of this 16:0-rich lipid from adult rats within 10 days correlates with the drastic loss of PUFA-rich GPL and VLCPUFA-rich SM and supports our interpretation that the latter, as seminolipids, were originally components of germ cells.

Along with saturated, monoenoic and dienoic fatty acids, the TG (TAG and alkyl-DAG) of rat testis initially contained PUFA of the n-6 series, particularly tetraenes with 20–28 carbon atoms and pentaenes with 22–32 carbon atoms. The main PUFA in both lipids were 22:5n-6, 24:4n-6, and 24:5n-6, all three being particularly high in alkyl-DAG, as shown previously [25]. Cryptorchidia caused a marked increase in the content and a change in the fatty acid composition of both neutral lipids, mainly evidenced by the accumulation of 22:5n-6. Previous work with rat seminiferous tubules has shown that [¹⁴C]24:4n-6 is actively desaturated to [¹⁴C]24:5n-6, and that both forms are actively esterified to TG, which suggest that these lipids rich in 24-C VLCPUFA may function as a dynamic chemical repository of PUFA [47]. Through chain shortening or 'retro-conversion,' 24:4n-6 and 24:5n-6 could be convenient and readily available sources of the major PUFA of the germ cell GPL 20:4n-6 and 22:5n-6. This hypothesis is supported by the fact that dietary modifications in the n-3:n-6 PUFA ratio arising from fish oil-rich diets result in relative deficiencies in n-6 fatty acids in mouse tissues and plasma [25]. This type of dietary pressure induced drastic depletion of both neutral glycerolipids and their n-6 PUFA from the testes, whereas the GPL retained their n-6 PUFA-rich pattern. Taken together, these observations support the idea that under normal conditions, TG may act as metabolically active donors of polyunsaturated acyl groups for the biosynthesis of PL, a markedly active process that is sustained throughout the adult life of the rat. When this synthesis is interrupted, as in the present model, the PUFA of TG are no longer able to play this role and thus they start to accumulate in these lipids. This would explain in part the increased amounts of PUFA, such as 22:5n-6, 24:4n-6, and 24:5n-6, in the TG. However, the selective accumulation of 22:5n-6 instead of other PUFA in the TG does not exclude the possibility that these lipids act as acceptors of fatty acids that originate from the breakdown of pre-existing GPL.

The CE of rat testis, which are shown in the present study to be rich in 22:5n-6 and VLCPUFA, particularly 28:5n-6 and 30:5n-6, belong to cells located within the seminiferous tubules [25], most probably Sertoli cells. These cells have a higher ratio of esterified to unesterified cholesterol than do germinal cells [19]. The fact that the VLCPUFA of adult CE are not observed in the testicular CE of sexually immature rats [25] strongly suggests they are involved in functions that appear after the onset of spermatogenesis. Under normal circumstances, one of these functions could be, as suggested for TG, to act as a temporary store of PUFA and VLCPUFA, which are precursors of polyenoic acyl chains, thus functioning as donors of PUFA with a biosynthetic role [25]. The behavior of CE

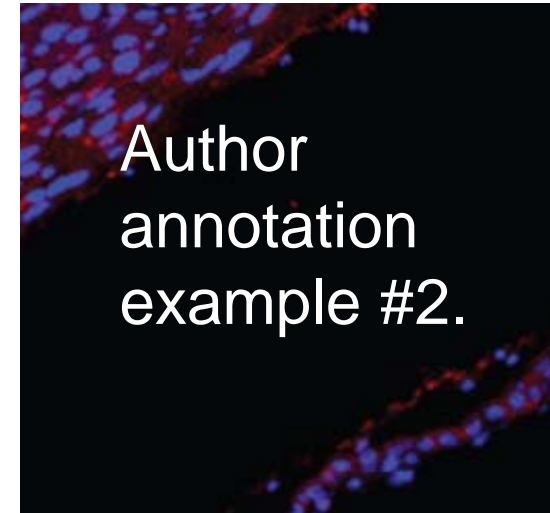
during cryptorchidism resembled that of the neutral glycerides, the massive accumulation of which suggests an even more direct relationship with the acyl groups of GPL. In this testicular condition, part of the PUFA of GPL seemed to end up as PUFA of TG and CE. It is possible that under stress circumstances similar to that in the present study, CE could act as a kind of temporary lipid buffer to protect the membranes of the surviving cells from the harmful accumulations of GPL-derived free fatty acids and free cholesterol formed in the membranes of dying cells.

It is interesting to note that as the amount of GPL formerly associated with the disappearing germ cells of cryptorchid testis decreased, TG and CE rich in PUFA tended to accumulate in the surviving cells, mostly Sertoli cells. Supporting evidence for the accumulation of neutral lipids in the latter may be found in the histologic observations presented by other authors, in which they show lipid droplets in the Sertoli cell cytoplasm under several pathological conditions that lead to spermatogenesis arrest [48, 49]. This is consistent with the fact that damaged or dead germ cells are phagocytosed by Sertoli cells, which hydrolyze and in some cases, reutilize some of the resulting elements [50–52].

Well-regulated cholesterol ester metabolism is essential for normal spermatogenesis, as revealed by the phenotype of hormone sensitive lipase (HSL)-deficient mice [53, 54]. In these mice, oligospermia is associated with CE accumulation owing to a complete lack of cholesterol ester hydrolase (CEH), an activity that is mediated by the testis-specific isoform of HSL. Durham and Grogan [55] characterized two isoforms of CEH in rat testes: a temperature-stable form and a temperature-labile form. The latter is present only in Sertoli cells and its activity is inhibited by a testicular temperature above 37°C [55, 56]. Interestingly, this form of the enzyme displays considerable substrate specificity, being less active towards CE with shorter (C16–18) fatty acids than towards CE with longer fatty acids (especially one with a very long chain, 24:1) [55]. Exposure of the testes to the abdominal temperature leads to a rapid inactivation of this thermolabile isoform of the CEH [56, 57]. Moreover, 4 days of cryptorchidism in rats leads to reductions in HSL activity, as well as in the amounts of HSL mRNA and protein [58]. The effect of cryptorchidism on this enzyme may explain the rapid increases in the amounts and concentrations of testicular CE observed in the present study.

The marked increase of testicular CE observed in cryptorchidism involved a moderate increase in its VLCPUFA compared to the dramatic and persistent increment in its 22:5n-6 and 20:4n-6. If VLCPUFA are precursors of PUFA after CE hydrolysis via chain shortening, they may accumulate in CE because they are no longer required. Since 22:5n-6, followed by 20:4n-6, were the PUFA that decreased the most in GPL, they could have accumulated in the CE as a way of protecting the surviving cells and/or preserving the polyenoic acyl chains. Since the accumulation of CE results either from the inhibition of CE hydrolase or from the stimulation of CE esterase activities, the dual behavior of the main VLCPUFA and PUFA of CE in the cryptorchid rat testis suggests that both systems are active in this 10-day period. These possibilities are not mutually exclusive.

The cryptorchid model, which represents an experimental situation that induces selective death of germ cells and survival of somatic cells (accumulating the neutral lipids TG and EC), allows discrimination of the main lipids of the major groups of cells in the rat seminiferous epithelium. Whereas 22:5n-6-rich glycerophospholipids and VLCPUFA-rich sphingolipids, as the 16:0-rich seminolipids, are tied to the fate of germ cells, the



Author
annotation
example #2.

Hmmm...

bor_77_01_20_162_169.056556IM.pdf - Adobe Acrobat Professional

File Edit View Document Comments Forms Tools Advanced Window Help

87.4%

Sticky Note Text Edit

TESTICULAR LIPIDS IN CRYPTORCHIDISM

enzymes involved in the synthesis of seminolipid or of its immediate precursor result in impaired spermatogenesis [45, 46]. Cerebroside sulfotransferase (CST)-null mice, generated by gene targeting, have been used to show that the same enzyme is involved in the synthesis of both brain sulfogalactosylceramide and testicular seminolipid [46]. ~~Cst(-/-) mice lack the former lipid in the brain and the latter lipid in the testis. Notably, whereas Cst(-/-) mice of both sexes show neurological abnormalities, only the males are infertile due to a block in spermatogenesis before the first meiotic division [46], which underlines the essential nature of seminolipid in normal spermatogenesis. In the present study, the fact that cryptorchidism induced the total loss of this 16:3-rich lipid from adult rats within 10 days correlates with the drastic loss of PUFA-rich GPL and VLCPUFA-rich SM and supports our interpretation that the latter, as seminolipids, were originally components of germ cells.~~

Across the saturated, monoenoic and dienoic fatty acids, the TG (TAG and DAG) of rat testis initially contained PUFA of the n-6 series, particularly tetraenes with 20-28 carbon atoms and pentaenes with 22-32 carbon atoms. The main PUFA in both lipids were 22:5n-6, 24:4n-6, and 24:5n-6, all three being particularly high in alkyl-DAGs as shown previously [25]. Cryptorchidism caused a marked increase in the content and a change in the fatty acid composition of both neutral lipids, mainly evidenced by the accumulation of 22:5n-6. Previous work with rat seminiferous tubules has shown that ¹⁴C[24:4n-6] is actively desaturated to ¹⁴C[24:5n-6], and that both forms are actively esterified to TG, which suggest that these lipids rich in 24-C VLCPUFA may function as a dynamic chemical repository of PUFA [47]. Through chain shortening or "retro-conversion," 24:4n-6 and 24:5n-6 could be convenient and readily available sources of the major PUFA of the germ cell GPL 20:4n-6 and 22:5n-6. This hypothesis is supported by the fact that dietary modifications in the n-3:n-6 PUFA ratio arising from fish oil-rich diets result in relative deficiencies in n-6 fatty acids in mouse tissues and plasma [25]. This type of dietary pressure induced drastic depletion of both neutral glycerolipids and their n-6 PUFA from the testes, whereas the GPL retained their n-6 PUFA-rich pattern. Taken together, these observations support the idea that under normal conditions, TG may act as metabolically active donors of polyunsaturated acyl groups for the biosynthesis of PL, a markedly active process that is sustained throughout the adult life of the rat. When this synthesis is interrupted, as in the present model, the PUFA of TG are no longer able to play this role and thus they start to accumulate in these lipids. This would explain in part the increased amounts of PUFA, such as 22:5n-6, 24:4n-6, and 24:5n-6, in the TG. However, the selective accumulation of 22:5n-6 instead of other PUFA in the TG does not exclude the possibility that these lipids act as acceptors of fatty acids that originate from the breakdown of pre-existing GPL.

The CE of rat testis, which are shown in the present study to be rich in 22:5n-6 and VLCPUFA, particularly 28:5n-6 and 30:5n-6, belong to cells located within the seminiferous tubules [25], most probably Sertoli cells. These cells have a higher ratio of esterified to unesterified cholesterol than do germinal cells [19]. The fact that the VLCPUFA of adult CE are not observed in the testicular CE of sexually immature rats [25] strongly suggests they are involved in functions that appear after the onset of spermatogenesis. Under normal circumstances, one of these functions could be, as suggested for TG, to act as a temporary store of PUFA and VLCPUFA, which are precursors of biosynthetic acyl chains, thus functioning as donors of PUFA with a biosynthetic role [25]. The behavior of CE during cryptorchidism resembled that of the massive accumulation of which our direct relationship with the acyl group in testicular condition, part of the PUFA of CE as PUFA of TG and CE. It is possible circumstances similar to that in the present as a kind of temporary lipid "buffer" to protect the surviving cells from the harmful acyl-derived free fatty acids and free cholesterol membranes of dying cells.

It is interesting to note that the amount of GPL form associated with the disappearing germ cells of cryptorchidism decreased, TG and CE rich in PUFA tend to accumulate in the surviving cells, mostly Sertoli cells. Supporting evidence for the accumulation of neutral lipids in the later may be found in the histologic observations presented by other authors in which they show lipid droplets in Sertoli cell cytoplasm that lead to sperm with the fact that by Sertoli cells, some of the results.

Well regulated normal spermatogenesis is highly sensitive to these mice, oligosaccharide chains, and glycoproteins, an activity that HSL, Durham and Vogelstein) stimulated in CEH in rat testes: a temperature-stable form and labile form. The latter is present only in Sertoli cells and its activity is inhibited by a testicular temperature at 56°C. Interestingly, this form of the enzyme displays substrate specificity, being less active towards shorter (C16-18) fatty acids than towards CE w/ acids (especially one with a very long chain). Exposure of the testes to the abdominal temperature led to rapid inactivation of this thermolabile isoform of HSL. Moreover, 4 days of cryptorchidism in rats led to reductions in HSL activity, as well as in the amount of mRNA and protein [58]. The effect of cryptorchidism on HSL enzyme may explain the rapid increases in the amount of testicular CE observed in the present study.

The marked increase of testicular CE observed in cryptorchidism involved a moderate increase in its VLCPUFA compared to the dramatic and persistent increment of 22:5n-6 and 20:4n-6. If VLCPUFA are precursors of CE after CE hydrolysis via chain shortening, they may accumulate in CE because they are no longer released, followed by 20:4n-6, were the PUFA of the GPL, they could have accumulated in the surviving cells and/or protected the acyl chains. Since the accumulation of VLCPUFA in CE in the cryptorchid rat testis is active in this 10-day period, not mutually exclusive.

The cryptorchid model, which represents a situation that induces selective death of somatic cells (accumulating the neutral lipids TG and EC), allows discrimination of the main lipids of the major groups of cells in the rat seminiferous epithelium. Whereas 22:5n-6-rich glycerophospholipids and VLCPUFA-rich glycerolipids, as the 16:3-rich seminolipids, are tied to the fate of germ cells, the

replace hyphen with space

delete and close up

suggesting

Inverted Text

Cross-Out

delete and close up

are also able to

that will eventually become the acyl groups of GPL [25]. Although

delete and close up

are formed

delete and close up

are able to

Inverted Text

Inverted Text

note only.

SM and Cer

Review & Comment

7 / 9

Start Outlook Today - Micro... Eudora - [In] Biology of Reproductio... Eudora - [Review Req... RevBatch 05.18.07 bor_77_01_20_16... Microsoft PowerPoint...

3:58 PM

...Ah!

cretary pressure induced drastic depletion of both neutral glycerolipids and their n-6 PUFA from the testes, whereas the GPL retained their n-6 PUFA-rich pattern. Taken together, these observations support the idea that under normal conditions, TG may act as metabolically active donors of polyunsaturated acyl groups for the biosynthesis of PL, a markedly active process that is sustained throughout the adult life of the rat. When this synthesis is interrupted, as in the present model, the PUFA of TG are no longer able to play this role and thus they start to accumulate in these lipids. This would explain in part the increased amounts of PUFA, such as 22:5n-6, 24:4n-6, and 24:5n-6, in the TG. However, the selective accumulation of 22:5n-6 instead of other PUFA in the TG does not exclude the possibility that these lipids act as acceptors of fatty acids that originate from the breakdown of pre-existing GPL.

The CE of rat testis, which are shown in the present study to be rich in 22:5n-6 and VLCPUFA, particularly 28:5n-6 and 30:5n-6, belong to cells located within the seminiferous tubules [25], most probably Sertoli cells. These cells have a higher ratio of esterified to unesterified cholesterol than do germinal cells [19]. The fact that the VLCPUFA of adult CE are not observed in the testicular CE of sexually immature rats [25] strongly suggests they are involved in functions that appear after the onset of spermatogenesis. Under normal circumstances, one of these functions could be, as suggested for TG, to act as a temporary store of PUFA and VLCPUFA, which are precursors of polyenoic acyl chains, thus functioning as donors of PUFA with a biosynthetic role [25]. The behavior of CE

rapid inactivation of this thermolabile isoform of the CEH [56, 57]. Moreover, 4 days of cryptorchidism in rats leads to reductions in HSL activity, as well as in the amounts of HSL mRNA and protein [58]. The effect of cryptorchidism on this enzyme may explain the rapid increases in the amounts and concentrations of testicular CE observed in the present study.

The marked increase of testicular CE observed in cryptorchidism involved a moderate increase in its VLCPUFA compared to the dramatic and persistent increment in its 22:5n-6 and 20:4n-6. If VLCPUFA are precursors of PUFA after CE hydrolysis via chain shortening, they may accumulate in CE because they are no longer required. Since 22:5n-6, followed by 20:4n-6, were the PUFA that decreased the most in GPL, they could have accumulated in the CE as a way of protecting the surviving cells and/or preserving the polyenoic acyl chains. Since the accumulation of CE results either from the inhibition of CE hydrolase or from the stimulation of CE esterase activities, the dual behavior of the main VLCPUFA and PUFA of CE in the cryptorchid rat testis suggests that both systems are active in this 10-day period. These possibilities are not mutually exclusive.

The cryptorchid model, which represents an experimental situation that induces selective death of germ cells and survival of somatic cells (accumulating the neutral lipids TG and EC), allows discrimination of the main lipids of the major groups of cells in the rat seminiferous epithelium. Whereas 22:5n-6-rich glycerophospholipids and VLCPUFA-rich sphingolipids, as the 16:0-rich seminolipids, are tied to the fate of germ cells, the

Expand All Collapse All Next Previous Reply Delete Set Status Checkmark Show Sort By Search Print Comments Options

	aa
Mel	suggests
	aa
Mel	note only
	aa
Mel	in
	pe
Mel Replacement Text 10/2/2007 4:00:26 PM	activities, which are not mutually exclusive, are operative in this 10-day period.
	aa
Mel	delete and close up
	aa
Mel	SM and Cer
	aa
Mel	delete and close up
	pe

Tricks & Tips

- Make it clear: stick with the best-practice mark-up basics
- Cut-and-paste
- Use html tagging when appropriate, for example:

89 ± 5 ng/10⁵ cells
for

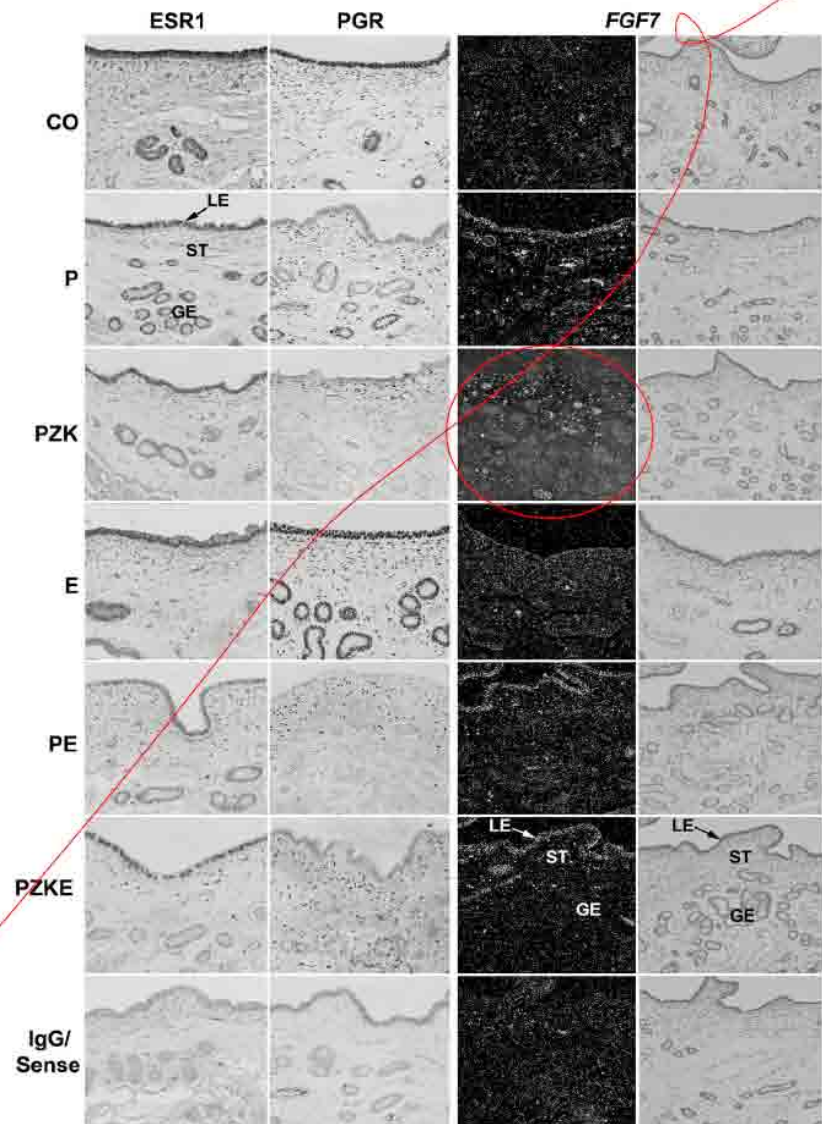
89 ± 5 ng/10⁵ cells

Pencil, highlight, arrow

Research Council (ARC) Ce
 'bourne, and ARC Centre o.

testes, i.e., PL depletion and CE accumulation, which lend support to the present conclusions. Cryptorchidism resulted in the fastest cellular and lipid biochemical changes (days as opposed to weeks). One important difference is that spermatogonia are preserved for some time in cryptorchidism, while they are damaged irreversibly and rapidly die in the other two models. If cryptorchidism is not corrected, the three situations have in common that they eventually lead to testicular involution and atrophy. If cryptorchidism is treated with adequate and rapid surgical correction, the surviving spermatogonia are potentially able to reinitiate spermatogenesis, and the testis may be eventually repopulated by spermatogenic cells. Although it may be predicted that the changes observed in the present study for testicular lipids are potentially reversible if the cryptorchid testis is replaced into its normal position, this is difficult to assess experimentally, as it would require further surgical manipulation of the animals. Since the cellular and biochemical effects conferred by this condition

REGULATION OF FGF7 IN THE PORCINE UTERUS



Other tips

- F8/F9 toggle
- Extract Pages
- Zoom shortcuts (Ctrl + “1” and “2”)
- Search feature
- Customize your toolbar (generic tip)
- Loupe and Snapshot
- Side-by-Side comparison

Side-by-Side Proofs

generate biotin-labeled cRNA
tion reaction, followed by in
TP. Ten micrograms of cRNA
s. The hybridized arrays were
l on the Affymetrix Scanner
ected for defects and quality.
ensity or major defects within
The final numbers of arrays
gments and six, five, six, and

Chip Operating System 1.0
ript expression values were
of 100. The default GCOS
Signal values and absolute
Analyst 3.0 (Genedata, Basle,

to be detectable if their mean
han 50 signal units and the
etermined by the GCOS default
samples within a group. Such
rs. Normalized signal values
comparative analysis of the
ualifier was considered to be
e qualifier was detected in
gments analyzed; and 2) a
elch test) existed between the
ese conditions were used for
expression values for each
standard deviation of 1 (z-
son of patterns within the data

TACCAGAGA-3', 5'-CCAAGGAGTTCAAGTTCAGACAGCCCA-3', and 5'-
CCCAGCACCTCGACGTTCT-3'; for *Gpx3* (NM_022525), 5'-TTGAACT-
GAATGCACTACAAGAAGAA-3', 5'-TTGGCCATTTCGGCCTGGTC-3',
and 5'-TGCAAGGGAAGCCAGAA-3'; for *Cst8* (NM_019258), 5'-AA-
GACACTCCATGCCACACT-3', 5'-TGCGGGAGACTTGAACATCA-3',
and 5'-CAGATCACAGACCGCATGGAATACCACA-3'; for *Defbl*
(NM_031810), 5'-TCTTGGACGCAGAACAGATCA-3', 5'-CAGCTGGA-
CGGAGACAGA-3', and 5'-TACCGATGCCTCCAAAATGGAGG-3'; for
Srd5a1 (NM_017070), 5'-CTTGACCCAGTTTGGCGTTT-3', 5'-TGCTGAA-
GACTGGGTGACCCATCCC-3', and 5'-TGCTGAAGACTGGGTGACC-
CATCCC-3'; for *Pepp1* (NM_017236), 5'-GGTTACAGCTCTA
GGATGCTTCCA-3', 5'-TGATAAGCCACCCAAAAG-3', and 5'-
TTTGTCAGGACCAGGCCAGTAACA-3'; for *Len5* (NM_024136), 5'-
GAGATTGCCTTTGCCTCCAA-3', 5'-CACCATGGCTCCCATCTTCT-3',
and 5'-ACACTGGCTTGGCACACAAGGA-3'; and for *Sod1*
(NM_017050), 5'-CGGATGAAGAGAGGCATGTTG-3', 5'-TTGGCCA-
CACCGTCTTT-3', and 5'-AGACCTGGGCAATGTGGTGCTG-3'.

Real-Time RT-PCR Analyses

Briefly, mRNA from each epididymal segment was analyzed by RT-PCR using 2.5 ng of total RNA in a final volume of 25 μ l that contained 300 nM of the target-specific PCR primers (Invitrogen, Carlsbad, CA), 100 nM fluorescently-labeled oligonucleotide probe (Eurogentec, San Diego, CA), and 1 \times Quantitect Probe RT-PCR Mix (Qiagen). Reverse transcription was performed for 30 min at 48°C, followed by 40 thermal cycles of 30 sec at 94°C and 1 min at 60°C using the 7900HT Fast Real-Time PCR System (Applied Biosystems). Target mRNA was normalized to 18S ribosomal RNA, as determined using TAQMANTM Ribosomal RNA Control Reagents (Applied Biosystems).

RESULTS

The segmentation of the proximal caput epididymis of the rat was evident under epi-illumination (Fig. 1A). EDL reduced

nsburg, MD). The tissues
PowerGen 700 automatic
A was extracted according
rified through RNeasy
reated with DNase on the
by the absorbance at 260
y was assessed using the

erate biotin-labeled cRNA
reaction, followed by in
Ten micrograms of cRNA
array (Affymetrix, Santa
The hybridized arrays were
n the Affymetrix Scanner
ed for defects and quality.
ty or major defects within
e final numbers of arrays
ents and six, five, six, and

ip Operating System 1.0
t expression values were
100. The default GCOS
nal values and absolute
lyst 3.0 (Genedata, Basle,

e detectable if their mean
50 signal units and the
ned by the GCOS default
ples within a group. Such
Normalized signal values
mparative analysis of the
fier was considered to be
e qualifier was detected in
gments analyzed; and 2) a
h test) existed between the
conditions were used for
pression values for each
standard deviation of 1 (z-
of patterns within the data

erate biotin-labeled cRNA
reaction, followed by in
Ten micrograms of cRNA
array (Affymetrix, Santa
The hybridized arrays were
n the Affymetrix Scanner
ed for defects and quality.
ty or major defects within
e final numbers of arrays
ents and six, five, six, and

ip Operating System 1.0
t expression values were
100. The default GCOS
nal values and absolute
lyst 3.0 (Genedata, Basle,

e detectable if their mean
50 signal units and the
ned by the GCOS default
ples within a group. Such
Normalized signal values
mparative analysis of the
fier was considered to be
e qualifier was detected in
gments analyzed; and 2) a
h test) existed between the
conditions were used for
pression values for each
standard deviation of 1 (z-
of patterns within the data

Real-Time RT-PCR Analyses

Briefly, mRNA from each epididymal segment was analyzed by RT-PCR using 2.5 ng of total RNA in a final volume of 25 μ l that contained 300 nM of the target-specific PCR primers (Invitrogen, Carlsbad, CA), 100 nM fluorescently-labeled oligonucleotide probe (Eurogentec, San Diego, CA), and 1 \times Quantitect Probe RT-PCR Mix (Qiagen). Reverse transcription was performed for 30 min at 48°C, followed by 40 thermal cycles of 30 sec at 94°C and 1 min at 60°C using the 7900HT Fast Real-Time PCR System (Applied Biosystems). Target mRNA was normalized to 18S ribosomal RNA, as determined using TAQMANTM Ribosomal RNA Control Reagents (Applied Biosystems).

RESULTS

The segmentation of the proximal caput epididymis of the rat was evident under epi-illumination (Fig. 1A). EDL reduced the size of the organ and made the appearance of the segment surfaces more indistinct (Fig. 1B). Segment histology showed significant reductions in lumen diameter and epithelial height (Fig. 1, C and D, Table 1), with the most marked changes in both features occurring in segment I (Table 1). The reductions in lumen diameter became progressively less severe as the segments become more distal, even in this very proximal part of the organ. Epithelial height reduction was also most

Trina	epididymis
aa	

Trina	expression

8.50 x 11.00 in

Review & Comment

3 / 8

8.50 x 11.00 in

Review & Comment

2 / 7

Start

Outlook Today...

Eudora - [In]

greatpowerpoint

Downloads

Eudora - [Review...

Final Rev Batch 0...

bor_77_01_19_1...

Search

bor_77_01_07...

bor_77_01_07_1...

Microsoft PowerP...

5:51 PM

Two-page layout with F8/F9 toggled

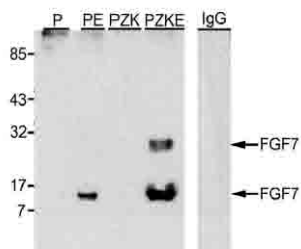


FIG. 2. Western blot analysis of FGF7 in porcine uterine luminal flushings. The positions of the prestained molecular mass standards are indicated. Immunoreactive FGF7 is detected (arrows) in the uterine flushings from ovariectomized pigs treated with P4 + E₂ (P4E2) or P4 + ZK + E₂ (P4ZKE2).

the stromal cells unresponsive to P4 (Fig. 4). Therefore, it seems likely that a progesteramin was not synthesized or released by stromal cells in response to P4 so as to mediate the induction of FGF7 mRNA in the LE of the 3/5 pigs that received both P4 and ZK.

Ovariectomized pigs treated with estradiol benzoate. The absence of P4 to down-regulate PGR and the effect of E₂ in inducing PGR resulted in the expression of PGR in the LE, which is considered to have prevented the induction of FGF7 mRNA in the LE by E₂ (Fig. 4).

Ovariectomized pigs treated with progesterone and E₂. Treatment of pigs with both P4 and E₂ allowed P4 to down-regulate the PGR in the LE and allowed E₂ to induce FGF7 mRNA expression in the endometrial LE (Fig. 3). Furthermore, the interaction of P4 with PGR in stromal cells probably allows the induction of a progesteramin that acts on the LE to induce the expression of FGF7 mRNA. Alternatively, the expression of FGF7 mRNA may be induced in this treatment group through a combination of these two mechanisms.

Ovariectomized pigs treated with progesterone, ZK, and E₂. The action of ZK on PGR in stromal cells inhibits the production of the putative progesteramin that is necessary for

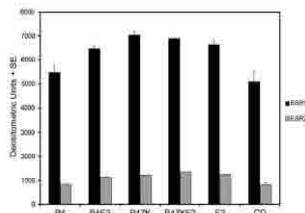


FIG. 3. RT-PCR analysis of ESR1 and ESR2 mRNAs in the endometria of pigs treated with P4, P4 + E₂ (P4E2), P4 + ZK (P4ZK), and P4ZKE2. Densitometric analyses of ESR1 and ESR2 transcripts from the endometria of pigs in different treatment groups following PCR amplification reveal that ESR1 mRNA is maintained at higher levels than ESR2 mRNA in all the treatment groups.

KA ET AL.

the induction of FGF7 expression in the LE (Fig. 4). Therefore, in the absence of functional PGR, E₂ action via ESR1 is considered to be sufficient for the induction of FGF7 mRNA expression in pig endometrial LE.

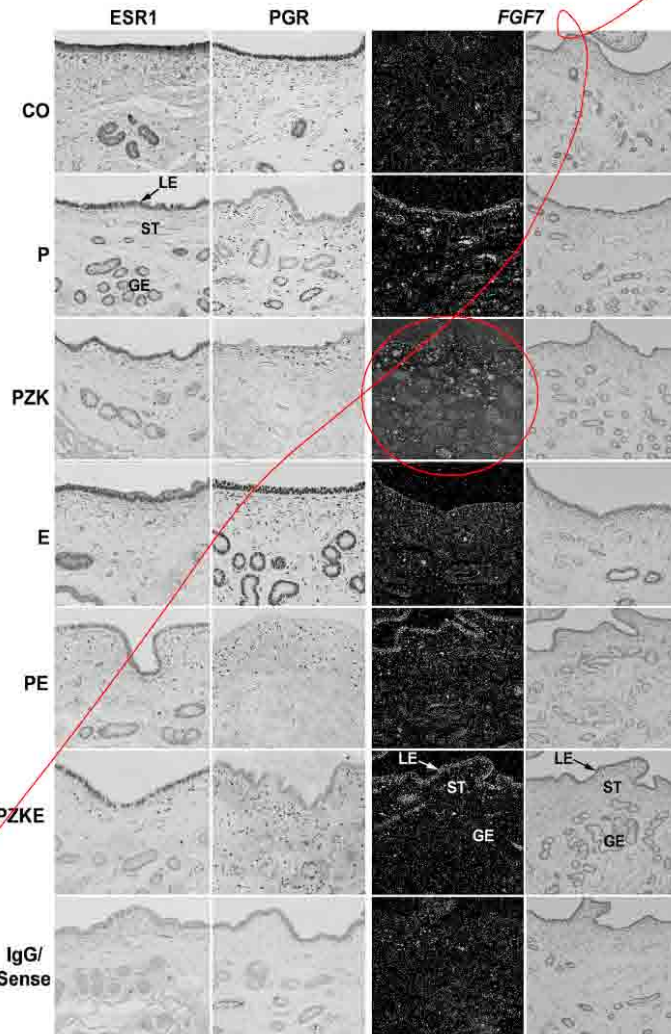
DISCUSSION

The results of the present study of pig endometria indicate that: 1) P4 is permissive for FGF7 expression through its action in down-regulating PGR in LE; 2) P4 stimulates PGR-positive uterine stromal cells to release an unidentified progesteramin, which induces FGF7 expression by the LE; 3) the combined effects of E₂ and P4 or E₂, P4, and ZK can induce FGF7 due to the effect of P4 in down-regulating PGR or the effect of ZK in blocking PGR function and allowing E₂ to act on PGR-negative LE; and 4) E₂ from conceptuses interacts via ESR1 in LE to induce maximal expression of FGF7 in PGR-negative LE on Day 12 of pregnancy in pigs. The group that received both P4 and E₂ is the most physiologically relevant, with P4 from the CL being permissive for the actions of E₂ from pig conceptuses during the peri-implantation period. A model that summarizes the present working hypothesis for hormonal regulation and the role of uterine FGF7 during early pregnancy in pigs is presented in Figure 5. The mechanism responsible for the lack of expression of FGF7 by endometrial GE is not known.

P4, which is the hormone of pregnancy in all mammals, is critical for the control of the temporal and spatial (cell-specific) changes in gene expression within the uterus that ensure synchrony between uterine and conceptus (embryo/fetus and associated membranes) development [31]. Indeed, treatment with exogenous P4 significantly alters the expression of a number of genes in rodent, primate, and sheep uteri, as measured in microarray analyses [32–34]. Although similar studies have not been performed in pigs, P4 increases the expression of calbindin-D9k [35], vascular endothelial growth factor [36], FGF2 and two of its receptors, FGFR1 and FGFR2 [37], and the α_4 , α_5 , and β_1 integrin receptor subunits [38], as well as suppressing the expression of MUC1 [38]. Importantly, P4 increases the expression levels of various uterine secretory proteins, components of the histotroph, which is hypothesized to support conceptus development in pigs [39–41]. Previous studies with endometrial explant cultures and in vivo steroid replacement experiments have failed to demonstrate FGF7 regulation by P4 in the pig uterus, since the investigators assumed that increases in FGF7 expression during the estrus

FIG. 4. Interrelationships between FGF7 mRNA, PGR protein, and estrogen receptor α protein in pig endometria. First column: nuclear localization of ESR1 protein in the luminal epithelia (LE) of corn oil (CO) and E₂-treated (E2) pigs, whereas PGR is present in stromal cells (ST) of the endometria from pigs in all the treatment groups. A section from an E₂-treated pig stained with nonimmune mouse IgG (IgG) serves as a negative control. The width of each field is 540 μ m. Second column: nuclear immunostaining for PGR in the LE, GE, and ST of endometria from pigs in all treatment groups. A section from an estradiol valerate-treated pig stained with nonimmune rat IgG serves as a negative control. The width of each field is 540 μ m. Third and fourth columns: in situ hybridization analysis of FGF7 mRNA expression in pig endometria. The left and right panels represent corresponding bright-field and dark-field images, respectively, of endometria from pigs in each treatment group. A representative section from a P4-treated pig hybridized with a radiolabeled sense cRNA probe (Sense) serves as a negative control. Note that FGF7 mRNA is detectable only in the LE, and that the hybridization signal is evident only in the endometria from pigs treated with P4, P4 + E₂ (P4E2), and P4 + ZK + E₂ (P4ZKE2). The width of each field is 690 μ m.

REGULATION OF FGF7 IN THE PORCINE UTERUS



Loupe tool

bor_77_01_12_69_77 056308HM.pdf - Adobe Acrobat Professional

File Edit View Document Comments Forms Tools Advanced Window Help

87.4% 100%

FIG. 2. Western blot analysis of FGF7 in porcine uterine luminal flushings. The positions of the prestained molecular mass standards are indicated. Immunoreactive FGF7 is detected (arrows) in the uterine flushings from ovariectomized pigs treated with P4 + E₂ (P4E2) or P4 + ZK + E₂ (P4ZKE2).

the stromal cells unresponsive to P4 (Fig. 4). Therefore, it seems likely that a progesteradin was not synthesized or released by stromal cells in response to P4 so as to mediate the induction of *FGF7* mRNA in the LE of the 3/5 pigs that received both P4 and ZK.

Ovariectomized pigs treated with estradiol benzoate. The absence of P4 to down-regulate PGR and the effect of E₂ in inducing PGR resulted in the expression of PGR in the LE which is considered to have prevented the induction of *FGF7* mRNA in the LE by E₂ (Fig. 4).

Ovariectomized pigs treated with progesterone and E₂. Treatment of pigs with both P4 and E₂ allowed P4 to down-regulate the PGR in the LE and allowed E₂ to induce *FGF7* mRNA expression in the endometrial LE (Fig. 3). Furthermore, the interaction of P4 with PGR in stromal cells probably allowed the induction of a progesteradin that acts on the LE to induce the expression of *FGF7* mRNA. Alternatively, the expression of *FGF7* mRNA may be induced in this treatment group through a combination of these two mechanisms.

Ovariectomized pigs treated with progesterone, ZK, and E₂. The action of ZK on PGR in stromal cells inhibits the production of the putative progesteradin that is necessary to

FIG. 3. RT-PCR analysis of *ESR1* and *ESR2* mRNAs in the endometria of pigs treated with P4, P4 + E₂ (P4E2), P4 + ZK (P4ZK), and P4ZKE2. Densitometric analysis of *ESR1* and *ESR2* transcripts from the endometria of pigs in different treatment groups following PCR amplification revealed that *ESR1* mRNA is maintained at higher levels than *ESR2* mRNA in all the treatment groups.

Treatment Group	ESR1 (Densitometric Units)	ESR2 (Densitometric Units)
P4	~600	~100
P4E2	~650	~100
P4ZK	~700	~100
P4ZKE2	~650	~100
E2	~600	~100
DO	~500	~100

is evident only in the endometria from pigs treated with P4, P4 + E₂ (P4E2), and P4 + ZK + E₂ (P4ZKE2). The width of each field is 690 μm.

550%

Start Outlook Today - Micro... Eudora - [In] Biology of Reproductio... Eudora - [Review Req... Rev Batch 05.18.07 bor_77_01_12_69... Microsoft PowerPoint -... 4:22 PM

Snapshot tool

KA ET AL.

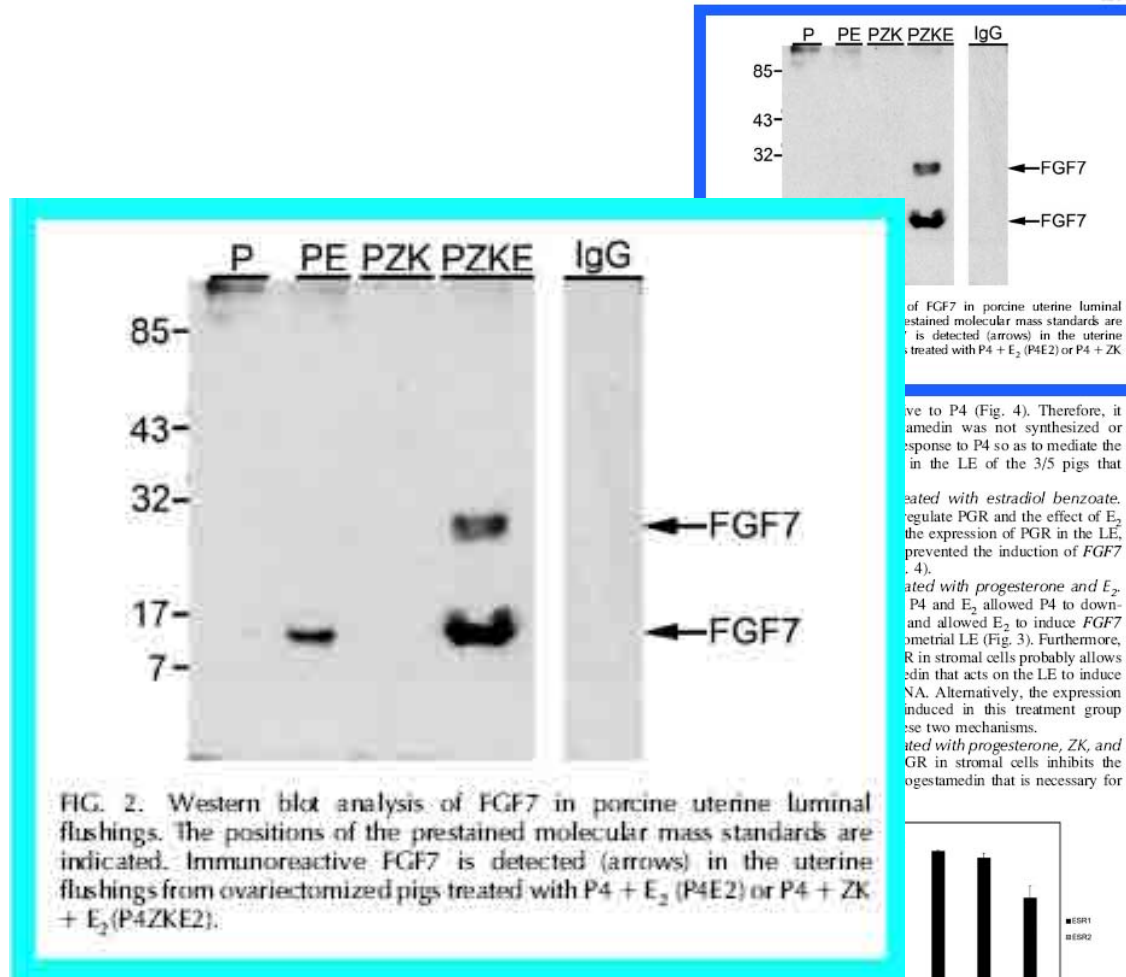


FIG. 2. Western blot analysis of FGF7 in porcine uterine luminal flushings. The positions of the prestained molecular mass standards are indicated. Immunoreactive FGF7 is detected (arrows) in the uterine flushings from ovariectomized pigs treated with P4 + E₂ (P4E2) or P4 + ZK + E₂ (P4ZKE2).

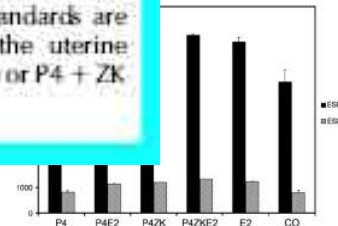


FIG. 3. RT-PCR analysis of *ESR1* and *ESR2* mRNAs in the endometria of pigs treated with P4, P4 + E₂ (P4E2), P4 + ZK (P4ZK), and P4ZKE2. Densitometric analysis of *ESR1* and *ESR2* transcripts from the endometria of pigs in different treatment groups following PCR amplification reveal that *ESR1* mRNA is maintained at higher levels than *ESR2* mRNA in all the treatment groups.

the induction of *FGF7* expression in the LE (Fig. 4). Therefore, in the absence of functional PGR, E₂ action via *ESR1* is considered to be sufficient for the induction of *FGF7* mRNA expression in pig endometrial LE.

DISCUSSION

The results of the present study of pig endometria indicate that: 1) P4 is permissive for *FGF7* expression through its action in down-regulating PGR in LE; 2) P4 stimulates PGR-positive uterine stromal cells to release an unidentified progestamin, which induces *FGF7* expression by the LE; 3) the combined effects of E₂ and P4 or E₂, P4, and ZK can induce *FGF7* due to the effect of P4 in down-regulating PGR or the effect of ZK in blocking PGR function and allowing E₂ to act on PGR-negative LE; and 4) E₂ from conceptuses interacts via *ESR1* in LE to induce maximal expression of *FGF7* in PGR-negative LE on Day 12 of pregnancy in pigs. The group that received both P4 and E₂ is the most physiologically relevant, with P4 from the CL being permissive for the actions of E₂ from pig conceptuses during the peri-implantation period. A model that summarizes the present working hypothesis for hormonal regulation and the role of uterine *FGF7* during early pregnancy in pigs is presented in Figure 5. The mechanism responsible for the lack of expression of *FGF7* by endometrial GE is not known.

P4, which is the hormone of pregnancy in all mammals, is critical for the control of the temporal and spatial (cell-specific) changes in gene expression within the uterus that ensure synchrony between uterine and conceptus (embryo/fetus and associated membranes) development [31]. Indeed, treatment with exogenous P4 significantly alters the expression of a number of genes in rodent, primate, and sheep uteri, as measured in microarray analyses [32–34]. Although similar studies have not been performed in pigs, P4 increases the expression of calbindin-D9k [35], vascular endothelial growth factor [36], *FGF2* and two of its receptors, *FGFR1* and *FGFR2* [37], and the $\alpha 4$, $\alpha 5$, and $\beta 1$ integrin receptor subunits [38], as well as suppressing the expression of *MUC1* [38]. Importantly, P4 increases the expression levels of various uterine secretory proteins, components of the histotroph, which is hypothesized to support conceptus development in pigs [39–41]. Previous studies with endometrial explant cultures and in vivo steroid replacement experiments have failed to demonstrate *FGF7* regulation by P4 in the pig uterus, since the investigators assumed that increases in *FGF7* expression during the estrus

FIG. 4. Interrelationships between *FGF7* mRNA, PGR protein, and estrogen receptor α protein in pig endometria. First column: nuclear localization of *ESR1* protein in the luminal epithelia (LE) of corn oil (CO) and E₂-treated (E2) pigs, whereas PGR is present in stromal cells (ST) of the endometria from pigs in all the treatment groups. A section from an E₂-treated pig stained with nonimmune mouse IgG (IgG) serves as a negative control. The width of each field is 540 μ m. Second column: nuclear immunostaining for PGR in the LE, GE, and ST of endometria from pigs in all treatment groups. A section from an estradiol valerate-treated pig stained with nonimmune rat IgG serves as a negative control. The width of each field is 540 μ m. Third and fourth columns: in situ hybridization analysis of *FGF7* mRNA expression in pig endometria. The left and right panels represent corresponding bright-field and dark-field images, respectively, of endometria from pigs in each treatment group. A representative section from a P4-treated pig hybridized with a radiolabeled sense cRNA probe (Sense) serves as a negative control. Note that *FGF7* mRNA is detectable only in the LE, and that the hybridization signal is evident only in the endometria from pigs treated with P4, P4 + E₂ (P4E2), and P4 + ZK + E₂ (P4ZKE2). The width of each field is 690 μ m.

Organizational Impact

- Online editing
- Everyone saves time
- Everyone saves money
- Big monitors

What's next...

- Procedures for authors to make them better annotators
- Explore e-tools for those who do not have the full Acrobat, e.g., FoxIt
- No more paper proofs!

A fluorescence microscopy image of a tissue section. The image shows a dense population of cells, with blue staining highlighting the nuclei and red staining highlighting specific cellular components or structures. The overall appearance is that of a histological section, possibly from a reproductive organ, given the context of the text.

Thank you for your kind attention!

Melissa Clifton, Deputy Managing Editor
Biology of Reproduction
mel@ssr.org